Two-Step Targeted Drug Delivery *Via* Proteinaceous Barnase-Barstar Interface and PLGA-Based Nano-Carrier

Victoria O. Shipunova (viktoriya.shipunova@phystech.edu)
Moscow Institute of Physics and Technology National Research University: Moskovskij fiziko-tehniceskij institut nacional'nyj issledovatel'skij universitet https://orcid.org/0000-0001-6361-1042

Elena N. Komedchikova
Moscow Institute of Physics and Technology: Moskovskij fiziko-tehniceskij institut nacional'nyj issledovatel'skij universitet

Anna S. Sogomonyan
Shemyakin-Ovchinnikov Institute of Bioorganic Chemistry Russian Academy of Sciences: FBGUN Institut bioorganiceskoj himii im akademikov M M Semakina i U A Ovcinnikova Rossijskoj akademii nauk

Polina A. Kotelnikova
Shemyakin-Ovchinnikov Institute of Bioorganic Chemistry Russian Academy of Sciences: FBGUN Institut bioorganiceskoj himii im akademikov M M Semakina i U A Ovcinnikova Rossijskoj akademii nauk

Maxim P. Nikitin
Moscow Institute of Physics and Technology: Moskovskij fiziko-tehniceskij institut nacional'nyj issledovatel'skij universitet

Sergey M. Deyev
Shemyakin-Ovchinnikov Institute of Bioorganic Chemistry Russian Academy of Sciences: FBGUN Institut bioorganiceskoj himii im akademikov M M Semakina i U A Ovcinnikova Rossijskoj akademii nauk

Research Article

Keywords: cancer, toxicity, nanoformulations, cytotoxicity

Posted Date: November 12th, 2021

DOI: https://doi.org/10.21203/rs.3.rs-1029355/v1

Abstract

The conventional methods of treating cancer with chemo- and radiotherapy present plenty of serious problems, such as low therapeutic index and high systemic toxicity. The advanced cancer treatment strategies utilize nanoformulations of drugs that can enter a tumor due to the enhanced permeability and retention (EPR) effect. However, EPR fails in the treatment of several human diseases. Mainstream biomedical studies are focused on creating the drugs that would enter the tumor with higher effectiveness and require smaller doses for administration. A two-stage drug delivery system is an encouraging alternative solution. At first, the primary, non-toxic targeting module is delivered to the tumor cells, followed by injection of the second complementary targeting module at a considerably lower dose, thus decreasing systemic toxicity. To meet the challenge, we have developed a two-stage drug delivery system (DDS), mediated by the high-affinity binding of the Barnase*Barstar protein pair. Barnase and Barstar act as lego bricks linking the first and the second modules on the surface of the cancer cell. Barnase (12 kDa) is a natural ribonuclease from *Bacillus amyloliquefaciens*, while Barstar (10 kDa) is its natural inhibitor. The Barnase*Barstar is one of the strongest known protein*protein complexes with $K_{aff} = 10^{14}$ M^{-1} exhibiting extraordinarily stability in severe conditions. Artificial scaffold polypeptide DARPin9_29 genetically fused with Barstar served is a first module of the developed two-step DDS. DARPin9_29 (14 kDa) specifically recognizes the tumor marker HER2 overexpressed on human breast cancer cells. As a second module, a therapeutic nano-cargo was developed based on fluorescent polymer PLGA nanoparticles loaded with diagnostic Nile Blue dye and the chemotherapeutic drug doxorubicin. This nano-PLGA structure was covalently coupled to Barnase. We showed two-stage efficient labeling of HER2-overexpressing cancer cells using the first non-toxic module DARPin9_29-Barstar and the second toxic nano-module PLGA-Barnase. We demonstrated the doxorubicin-induced cytotoxicity of this two-step DDS based on polymer nanoparticles and proteinaceous Barnase-Barstar interface and showed more than 10-fold therapeutic dose reduction versus free doxorubicin. We believe that the developed two-step DDS based on PLGA nano-cargo and protein interface will promote the creation of new-generation cancer treatment strategies.

Introduction

Cancer is one of the most significant threats to humankind. In 2020 only, 19.1 million cases were registered, and this number is supposed to reach 28.4 million by 2040. It is the second most frequent death cause, and the contribution of cancer to the mortality rate continues to grow [1]. Conventional cancer therapy strategies suffer from a lack of selectivity and low drug efficiency and are frequently associated with side effects, including cardiac dysfunction, cytopenia, infection, diarrhea, vomiting, and others [2, 3].

Chemotherapy-loaded nanoparticles capable of increasing the amount of therapeutic drug that reaches the tumor site and reducing the systemic toxicity provide encouraging solutions to the described problems. Moreover, drug encapsulation into the nanoparticle architecture can increase the bioavailability

of the chemotherapeutic compound, extend the duration of action *via* bloodstream circulation prolongation, and can solve the problems associated with hydrophobicity and insolubility of drugs [4–8].

Several nanoparticle-based medications, such as PEGylated liposomal doxorubicin Caelyx® [9], and liposomal formulation of daunorubicin and cytarabine VYXEOS® [10], have already been approved by FDA for cancer treatment. However, despite the improved efficiency of such formulations, the delivery of nanoparticles occurs by passive transport through enlarged pores in the vascular endothelium of tumors known as the “enhanced permeability and retention (EPR)” effect [4]. However, it was shown that the EPR effect fails in some tumors and for some patients. Therefore, it is critical to develop different approaches for the delivery of nanoparticles to cancer cells [11]. One of the ways to implement targeted delivery is to modify the surface of nanoparticles with molecules binding certain cancer cell receptors. This is a rapidly developing branch of biomedicine that has already demonstrated several promising results in clinical trials [12, 13]. Various proteins, such as antibodies, transferrin, EGF, lectins, as well as protein-nucleic acid complexes, aptamers, and small molecules like folic acid and sugars, are traditionally used for targeted drug delivery [14]. Currently, small synthetic polypeptides (scaffold molecules) emerge as the most promising targeting compounds due to their remarkable affinity, stability, ease of biotechnological production, and the absence of immunomodulation *in vivo* [14–17].

A pre-targeting concept implying two-step delivery of therapeutic compounds to tumor site is expected to provide significant systemic nanoparticle toxicity reduction and nanoparticle targeting abilities improvement [18]. This concept is based on the initial delivery of the first targeting non-toxic compound to specific cancer cells in a moderately high dose (thus realizing pre-targeting) followed by the delivery of a relatively small dose of a second toxic compound interacting with the first one in a key&lock mode. A two-step drug delivery systems (DDS) offer a series of benefits over standard one-step systems, such as 1) reduced toxicity for normal cells; 2) controlled penetration of toxin into the tumor; 3) improved drug biodistribution; 4) reduction of the required dose of the drug [19]. The disadvantages of the currently available two-step DDSs are due to the immunogenicity of the components, possible competition with molecules in the bloodstream, and the expensive and time-consuming biotechnological production in mammals of the components of such DDSs [20, 21].

Here for the first time, we used Barnase*Barstar pair as a platform for two-stage delivery of the onco-therapeutic compound. Ribonuclease Barnase and its natural inhibitor Barstar are small proteins (12 and 10 kDa) of bacterial origin that are not presented in mammals and possess an extremely high constant of binding ($K_{aff} = 10^{14}$ M^{-1}). We synthesized polymer PLGA nanoparticles and loaded them with the chemotherapeutic drug doxorubicin and the fluorescent dye Nile Blue, and successfully modified the surface of nanoparticles with Barnase. The Barnase*Barstar interface was used as lego bricks to link the toxic PLGA nanoparticles with scaffold protein DARPin9_29 recognizing the tumor marker HER2 on the surface of cancer cells. DARPin9_29 was genetically fused with Barstar to obtain DARPin9_29-Barstar protein capable of specifically targeting HER2-overexpressing cancer cells. We showed two-stage efficient labeling of HER2-overexpressing cancer cells with supramolecular structure PLGA-Barnase*DARPin9_29-Barstar self-assembled on the cell surface. We demonstrated the cytotoxicity of nanoparticles and more

than tenfold therapeutic dose reduction versus free doxorubicin thus confirming the potential of this DDS for cancer treatment.

Materials And Methods

Nanoparticle synthesis

PLGA nanoparticles were synthesized by the double emulsion “water-oil-water” method, followed by solvent evaporation, according to a modified procedure developed by us earlier [22]. The first emulsion was obtained by adding 150 µL of an aqueous solution of doxorubicin hydrochloride at a concentration of 2 g/L to chloroform containing 300 µL of PLGA at a concentration of 40 g/L and 50 µL of Nile Blue at various concentrations, followed by sonication for 1 min at 40% amplitude and for 1 min at 60% amplitude using a 130 W ultrasonic disintegrator (Sonics) at +4°C. The second emulsion was created by mixing the first emulsion with 3 mL of 5% polyvinyl alcohol solution in milliQ with the addition of 1 g/L chitosan oligosaccharide lactate. The solution was sonicated for 1 min at 40% amplitude and 1 min at 60% amplitude at +4°C. The resulting solution was incubated with slow shaking for chloroform evaporation, then washed three times in PBS by centrifugation, and resuspended in 300 µL of PBS PBS (137 mM NaCl, 2.7 mM KCl, 4.77 mM $Na_2HPO_4 \cdot 2H_2O$, 1.7 mM KH_2PO_4, pH 7.4). The final concentration of nanoparticles was determined by drying at 60°C and followed by weighing the dry residue.

Electron microscopy

Electron microscopy images of PLGA particles were obtained with a MAIA3 (Tescan) microscope at an accelerating voltage of 15 kV. The samples were deposited onto a silicon wafer and then dried in the air. The resulting images were processed using ImageJ software to obtain a particle size distribution.

Particle size and surface charge measurements

The hydrodynamic sizes and ζ-potential of nanoparticles were determined in PBS at 25°C using a Zetasizer Nano ZS (Malvern Instruments Ltd.) analyzer.

Nanoparticles conjugation with proteins

Barnase and Barstar were expressed and purified as described by us previously[23]. PLGA nanoparticles were covalently modified with Barnase or Barstar proteins using EDC and s-NHS as cross-linking agents through the formation of amide bonds between amino groups on the particle surface and protein carboxyl groups. 200 µg of protein was activated by a 15-fold molar excess of EDC and s-NHS in 0.1 M MES, pH 5.0 for 40 min at room temperature. Then protein was added to 1 mg of PLGA nanoparticles in 1) borate buffer – 0.4 M H_3BO_3, 70 mM $Na_2B_4O_7 \cdot 10H_2O$, pH 8.0, 2) 0.1 M HEPES (4-(2-hydroxyethyl)-1-piperazineethanesulfonic acid) pH 6.0, and sonicated. The mixture was incubated for at least 5 hours at room temperature, periodically treated in an ultrasonic bath, and the unbound protein was washed off by triple centrifugation for 5 minutes at 8000 g, finally resuspending the particles in PBS with 1% BSA.

Measurement of Barnase activity

The RNAse activity of Barnase was investigated by the method of the acid-insoluble precipitate [24]. The protein solution or solution of nanoparticles in 40 µL of buffer (0.125 M Tris-HCl, pH 8.5) was mixed with 160 µL of yeast RNA at a concentration of 2 g/L and incubated at 37° C for 15 min. The reaction was terminated by the addition of 200 µL of 0.625 N H_2SO_4 and the mixture was incubated for 5 min at room temperature. Undigested RNA was separated by centrifugation at 14000 g for 15 min at room temperature. Optical density was measured at λ = 260 nm (OD260) corresponding to the concentration of free mononucleotides and proportional to the activity of the enzyme. The inhibition of Barnase RNAse activity was measured similarly: nanoparticles with Barstar were pre-incubated with 2.5 nM Barnase, and the enzymatic activity of the mixture was measured as described above.

Fluorescent microscopy

Excitation and emission spectra of PLGA nanoparticles were obtained using an Infinite M100 Pro (Tecan) microplate reader. Nanoparticle suspension at a concentration of 10 µg/mL in 100 µL of PBS was placed in a 96-well flat-bottomed plate. Excitation spectra were measured in the range from 350 to 675 nm (with the emission of 700 nm), emission spectra from 675 to 850 nm (excitation wavelength 650 nm).

Protein conjugation to FITC

Bn-DARPin9_29 was expressed and purified as described by us previously[25]. Bs-DARPin9_29 was expressed is follows. Freshly transformed *Escherichia coli* BL1 (DE3) strain was grown in ZYM-5052 autoinduction medium (2% tryptone, 1% yeast extract, 0.5% glycerol, 0.05% glucose, 0.02% lactose, 25mM Na_2HPO_4, 25mM KH_2PO_4, 50mM NH_4Cl, 5 mM Na_2SO_4, 2 mM $MgSO_{4[26]}$) containing 0.2 g/L ampicillin. The culture was grown in the thermostatic shaker at 25°C and 200 rpm overnight. Cells were harvested by centrifugation at 5000g for 15 min at 4 ºC. Cell pellets were resuspended in lysis buffer (20 mM Na-Pi, 300 mM NaCl, pH 7.4, 50 µg/mL lysozyme) and then sonicated on ice. Cellular debris was removed by centrifugation at 30000g at 4°C for 2 h. After the addition of imidazole (20 mM), the supernatant was filtered through a 0.22 µm membrane and applied onto a HisTrap HP, 1 mL column (GE Healthcare) equilibrated with 20 mM sodium phosphate buffer (pH 7.4), 300 mM NaCl and 20 mM imidazole. The bound proteins were eluted with imidazole step gradient (50, 75, 100, 150, 200, 250, and 500 mM). The fractions were analyzed by 15% reducing SDS- PAGE.

Proteins were conjugated to FITC as follows: 100 µg of protein in 90 µL of PBS was rapidly mixed with 10 µL of FITC in DMSO and incubated overnight at room temperature with an 8-fold molar excess of FITC to protein. Proteins were purified from unreacted FITC molecules using a Zeba Spin Desalting Columns, 7k MWCO (Pierce) according to the manufacturer's recommendations.

Cell culture

Cell lines – human breast adenocarcinoma, SK-BR-3, and Chinese hamster ovary, CHO, were cultured in DMEM medium supplemented with 10% fetal bovine serum, penicillin-streptomycin, and 2 mM L-glutamine. Cells were incubated in a humidified atmosphere with 5% CO2 at 37°C. Cells were passaged when they reached 80-90% of the monolayer. To remove cells from the surface of the plastic 2 mM EDTA

solution in PBS was used without trypsin addition (to avoid disruption of the integrity of cell receptors). Cell lines were maintained in culture for no more than 2 months, after which they were replaced with fresh frozen lines. For cell counting, a Countess (Invitrogen) automatic cell counter was used. For this, 5 µL of 0.4% trypan blue, which stains only dead cells, was added to 5 µL of cell suspension. The solution was pipetted and added to the slides for the automatic cell counting.

Flow cytometry

To determine the efficiency of cells labeling with FITC-modified proteins, the cell suspension was washed with PBS, resuspended in 300 µL of PBS with 1% BSA at a concentration of 10^6 cells/mL. Cells were labeled with proteins in a final concentration of 2 µg/mL, washed, and analyzed in FL1 channel (excitation laser – 488 nm, emission filter – 530/30 nm) using a BD Fortessa (BD) flow cytometer.

To determine the specificity of targeted nanoparticles, the cell suspension was washed in PBS, resuspended in 300 µL of PBS with 1% BSA at a concentration of 10^6 cells/mL.

Cells were incubated with Bs-DARPin9_29 at concentrations 0, 0.5 and 2.5 µg/mL for 1 hour at +4°C, washed from unbound protein by triple centrifugation. Then, PLGA-Bn conjugates were added to the cells, incubated for 15 min, and washed from unbound nanoparticles by double centrifugation. Samples were analyzed using a BD Accuri C6 (BD) flow cytometer in the FL4 detection channel (excitation laser – 644 nm, emission filter – 675/25 nm).

Fluorescent microscopy

Cell suspension at a concentration of 10^6 cells/mL in PBS with 1% BSA was labeled with proteins at the final concentration in the sample of 1 µg/mL on ice for 30 min, washed from unbound dyes by triple centrifugation, after which it was analyzed on glass slides using a camera Nuance N-MSI-500-FL on a Nikon TE200-U microscope in fluorescence channel corresponding to the FITC channel, and in transmitted light at the same exposure and brightness settings for all samples.

Cytotoxicity assay

Cytotoxicity of the synthesized nanoparticles and doxorubicin was investigated using a standard MTT-test. Cells were seeded in a 96-well plate at 10^4 cells per well in 100 µL of full DMEM with an addition of 10% FBS and cultured overnight. Then, test substances were added to the wells in 100 µL of DMEM and incubated for 72 hours. Next, the medium was removed, and 100 µL of MTT (tetrazolium dye 3-(4,5-dimethylthiazol-2-yl)-2,5-diphenyltetrazolium bromide) solution at a concentration of 0.5 g/L in DMEM was added to the cells. The samples were incubated for 1 hour at 37°C, the MTT solution was removed, and 100 µL of DMSO was added to the wells, the plate was moderately shaken until the formazan crystals were completely dissolved. The optical density of each well was measured with an Infinite M1000 Pro microplate analyzer (Tecan) at a wavelength of 570 nm and a reference wavelength of 630 nm. The viability of cells was presented in percent in comparison to the untreated sample. All samples were performed in triplicate. IC50 was calculated using GraphPad Prism software.

Results

Synthesis and characterization of polymer nanoparticles based on poly-(D, L-lactic-co-glycolic acid)

Poly-(D, L-lactic-co-glycolic acid) nanoparticles (PLGA) possessing both fluorescent and cytotoxic properties were synthesized by the double water-oil-water emulsion method as shown in Figure 1.

Nile Blue ([9-(diethylamino)benzo[a]phenoxazin-5-ylidene] azanium sulfate, also known as Nile Blue A) was incorporated in the nanoparticles as a fluorescent dye that allows to track the particles inside cells and use them for diagnostic purposes. This dye is successfully used in a wide range of biological applications, such as gel electrophoresis, staining of histological sections, labeling of neutral lipids and fatty acids, and visualization of cancer cells[27]. Nile Blue is a biocompatible dye with absorption and emission maxima in the near-infrared optical window (635 and 674 nm in water solution, respectively), which makes it optimal for labeling target cells *in vitro* and *in vivo*.

Doxorubicin was incorporated into the nanoparticles that allow using them for therapeutic applications. Doxorubicin is an anthracycline antibiotic, that causes cell death by the interaction with DNA and inhibition of topoisomerase II, which leads to suppression of nucleic acids synthesis, and by the formation of free radicals, that destroy cellular membrane and biomolecules [28, 29].

Nanoparticles were synthesized by the double emulsion “water-oil-water” method with subsequent evaporation of the solvent as shown in Figure 1.

The first emulsion was obtained by the addition of water doxorubicin solution to the solution of PLGA and Nile Blue in chloroform, followed by a short sonication. The second emulsion was obtained by the addition of the first emulsion to the polyvinyl alcohol solution containing 1 g/L of chitosan oligosaccharide lactate, followed by the second short sonication. After chloroform evaporation by the slow mixing, nanoparticles were centrifugated and resuspended in phosphate-saline solution (PBS).

The nanoparticles’ morphology was studied by scanning electron microscopy (MAIA3 microscope, Tescan) at an accelerating voltage of 15 kV using an in-beam secondary electron detector. The received images (Fig. 2a) illustrate that synthesized PLGA nanoparticles are spherical monodisperse structures. Image processing with ImageJ software shows that the average size and standard deviation of nanoparticles are 218 ± 59 nm (Fig. 2b). The hydrodynamic size of nanoparticles, measured by the dynamic light scattering method, was determined as 201 ± 38 nm (Fig. 2c) thus completely corresponding to the value of the physical size of nanoparticles. These data indicate that nanoparticles preserved colloidal stability and did not form aggregates in saline solution. Moreover, visual observation showed that nanoparticles were stable for at least 6 months; further observations were not carried out. The ζ-potential of nanoparticles, measured by the electrophoretic light scattering method, was –1.64 mV (Fig. 2d) thus slightly deviating from zero. Such surface charge at pH 7.4 was due to the presence of both

negatively charged carboxyl groups –COOH (within the composition of PLGA) and positively charged amino groups $–NH_2$ (within the composition of chitosan) on the surface of the nanoparticles.

The efficient incorporation of the fluorescent dye Nile Blue was investigated by fluorescence spectroscopy by measuring the excitation and fluorescence emission spectra of nanoparticles. The excitation spectra were measured in the range from 350 to 675 nm (with emission at 700 nm). Four PLGA nanoparticles with different Nile Blue concentrations used in the synthesis were investigated. The excitation spectra (Fig. 2e) and emission spectra (Fig. 2f) demonstrate that the most effective Nile Blue concentration during the synthesis is 1.7 g/L, the further scaling up of Nile Blue concentration leads to the decrease in fluorescence intensity. It is most probably caused by non-fluorescent H-aggregates formation having an absorption shifted to the blue region of the spectrum.

The efficient incorporation of doxorubicin was investigated by fluorescent spectroscopy on nanoparticles that do not contain Nile Blue. Nanoparticles were solved in DMSO and then fluorescence was measured using a fluorescence calibration curve for doxorubicin samples in the same solutions. The measurement of the fluorescence of the samples showed that doxorubicin incorporation was 0.9 nmol doxorubicin per 1 mg of nanoparticles.

Barnase*Barstar protein interface for the targeted two-step delivery of PLGA particles to HER2-overexpressing cancer cells

One of the central problems of modern chemotherapy is its relative non-specificity. The nanoparticle surface should be modified with targeting molecules in order to incorporate cancer cell targeting modalities into the nanoparticle structure and reduce non-specific toxicity to normal non-transformed cells. To make this kind of modification universal for any target on the cell surface and include the possibility to "cancel the action on demand”, we propose to mediate the interaction between toxic nanoparticles and molecules recognizing cancer cells using protein adaptors, the Barnase*Barstar protein pair. Barstar (10 kDa) is a natural inhibitor of bacterial ribonuclease Barnase (12 kDa) [23]. The N- and C-terms of both proteins are available for chemical conjugation and genetic engineering and are not located in the active site of both enzymes.

We used scaffold protein DARPin9_29 that recognizes the receptor HER2 on the surface of cancer cells with high affinity (K_D = 3.8 nM) for the targeted delivery of synthesized polymer PLGA nanoparticles to cancer cells. This modular DDS based on PLGA nanoparticles, protein adaptors Barnase*Barstar, and scaffold proteins are schematically illustrated in Figure 3.

The surface of the nanoparticles was modified by one of the components of the pair – Figure 3 shows PLGA nanoparticles covalently modified with Barnase. During the pre-targeting process, Barstar-DARPin9_29 bifunctional protein was added to the cells with HER2 overexpression lading to the selective binding of the anti-HER2 molecule to the cancer cell surface. Next, self-assembly with the second component of the pair was carried out, namely, with PLGA nanoparticles conjugated with Barnase. The

resulting supramolecular structure selectively interacted with the cells with overexpression of receptor HER2: DARPin9_29 mediated the internalization of PLGA nanoparticles in the cells, while chemotherapy drug induced cell death.

Chemical modification of PLGA nanoparticles was carried out by using the sodium salt of 1-ethyl-3- (3-dimethyl aminopropyl) carbodiimide, EDC, and the sodium salt of N-hydroxysulfosuccinimide, s-NHS, as cross-linking agents through the formation of amide bonds between the carboxyl groups of proteins and amino groups on the surface of nanoparticles. In the first stage of the reaction, proteins were activated with EDC/s-NHS mixture in an acidic buffer with pH 5.0, then nanoparticles were added to the buffer with pH 6.0 or pH 8.0.

The efficiency of conjugation was measured by the enzymatic ability of conjugated nanoparticles to hydrolyze RNA by the commonly used method of the acid-insoluble precipitate [24]. First, the solution of conjugated PLGA nanoparticles was mixed with yeast RNA and incubated at 37°C to digest RNA. Then, the reaction was stopped by the addition of sulfuric acid, and uncleaved RNA was separated by centrifugation. The optical density of the solution corresponding to the concentration of free mononucleotides and proportional to the activity of the enzyme was measured. This value is proportional to the ribonuclease activity of the tested proteins or nanoparticles. The inhibition of RNAse activity of Barnase was measured similarly. Nanoparticles with Barstar were pre-incubated with Barnase, and the enzymatic activity of the mixture was measured as described above.

The enzymatic activity of free Barnase and Barstar proteins is shown in Figure 4a. The purple curve corresponds to the activity of the free Barnase and has a concentration-dependent manner achieving saturation. As a positive control in the experiment directed to the investigation of the enzymatic activity of PLGA nanoparticles conjugated with Barnase, a sample with Barnase at a concentration of 2.5 nM was used. This point corresponds to the middle of the linear range of the Barnase enzymatic activity curve. The enzymatic activity of Barstar, namely the ability to inhibit Barnase, was investigated similarly by its pre-incubation with 2.5 nM of Barnase (green curve in Figure 4a) and measuring the enzymatic activity of the sample. As a positive control in the investigation of the enzymatic activity of PLGA nanoparticles conjugated with Barstar, a sample with Barstar at a concentration of 15 nM (+ Barnase 2.5 nM) was used.

We obtained three types of PLGA nanoparticles modified with Barnase by three different methods: i) carbodiimide conjugation at pH 8.0, ii) carbodiimide conjugation at pH 6.0, iii) non-covalent protein adsorption on the particle surface. Data presented in Figure 4b indicate that the highest efficiency of modification of PLGA nanoparticles is achieved during chemical conjugation at pH 6.0. Similar data were obtained for PLGA nanoparticles conjugated with Barstar: the highest inhibition of the Barnase activity is achieved for conjugates obtained at pH 6.0. Therefore, the possibility of obtaining functionally effective PLGA nanoparticles in terms of enzymatic activity with both Barnase and Barstar has been demonstrated.

2.3. Targeted delivery of polymer PLGA nanoparticles to the cells with oncomarker HER2 overexpression

One of the options, displayed in Figure 3 was employed to demonstrate the efficiency of the proposed scheme for the creation of targeted nanostructures for delivery to the cancer cells for their selective destruction. Namely, conjugates of PLGA nanoparticles with Barnase, PLGA-Bn, were obtained, and self-assembled on the cancer cell surface using Barstar fused with DARPin9_29. Thus, supramolecular structures PLGA-Bn*Bs-DARPin9_29 were assembled on the cell surface using pre-targeting concept via Bs-DARPin9_29 protein and subsequent binding with PLGA*Bn. These structures were delivered to the cells overexpressing receptor HER2.

For the *in vitro* experiments, we selected two cell lines with various levels of HER2 expression, namely SK-BR-3 and CHO cells. SK-BR-3 is a mammary adenocarcinoma cell line with overexpression of HER2 (about 10^6 receptors per cell), while CHO, Chinese hamster ovary cells, do not express any receptor of the EGFR family. Expression of HER2 receptor on these cells was confirmed by confocal microscopy (Fig. 5a) and by flow cytometry (Fig. 5b) by imaging cells with fluorescence-labeled full-length antibody against HER2 – Trastuzumab-FITC. Also, the binding of DARPin9_29 was confirmed by cell labeling with DARPin9_29-FITC (Fig. 5b). Data from microscopy and cytometry assays presented in Figure 5a,b indicate that SK-BR-3 cells do express HER2 and are effectively labeled with full-length anti-HER2 antibody Trastuzumab and anti-HER2 scaffold protein DARPin9_29.

The functional activity of DARPin within the composition of fusion proteins with Barnase and Barstar – Bn-DARPin9_29 and Bs-DARPin9_29 was confirmed by flow cytometry (Fig. 5b) by labeling cells with overexpression of receptor HER2. It was demonstrated that the presence of Barnase and Barstar in fusion protein does not affect the interaction of DARPin9_29 with HER2-positive cells. Thus, both components of the Barnase*Barstar protein pair did not influence the functional activity of recognizing scaffold DARPin9_29 and can be used as adaptor proteins mediating two-step targeted drug delivery.

The functional polymer PLGA nanostructures were used for selective targeting of cells with HER2 overexpression. Labeling was carried out by the two-stage targeted delivery method. At the first stage, cells were incubated in suspension with Bs-DARPin9_29 in two different concentrations, followed by washing from unbound protein. Next, the cells were labelled by PLGA-Bn, followed by washing from unbound particles. The binding between nanostructures and cells was estimated by flow cytometry with excitation with a 640 nm laser in the fluorescence channel corresponding to the Nile Blue fluorescence.

The data presented in Fig. 5c indicates highly efficient labeling of HER2-overexpressing cells by polymer PLGA nanostructures, assembled on the cells' surface, PLGA-Bn*Bs-DARPin9_29. Non-specific labeling of cells by PLGA-Bn conjugates is not observed, and binding of PLGA-Bn*Bs-DARPin9_29 with cells has a concentration-dependent manner. With an increase in the concentration of Bs-DARPin9_29 by 5 times from 0.5 μg/mL to 2.5 μg/mL, the median fluorescence intensity of the cell population increases by 17551/2904 = 6 times.

Cytotoxicity of targeted supramolecular structures PLGA Bn*Bs DARPin9_29

Along with a fluorescent dye, the synthesized PLGA polymer nanoparticles contain a chemotherapeutic drug, doxorubicin, which induces cell death *via* apoptosis. The cytotoxicity of PLGA-Bn*Bs-DARPin9_29 nanostructures was investigated by standard MTT test three days after adding the nanostructures in different concentrations to the HER2-overexpressing cells. The therapeutic effectiveness of targeted nanostructures was compared with free doxorubicin, which was added to the cells under similar conditions, as well as non-targeted PLGA nanoparticles loaded with doxorubicin.

The results of the cytotoxicity study of targeted PLGA nanoparticles with doxorubicin and free doxorubicin are presented in Fig. 5d, which shows the molar concentration of free doxorubicin and molar concentration of doxorubicin incorporated inside PLGA particles.

Half-maximal inhibitory concentration (IC50) was calculated for doxorubicin, PLGA, and PLGA-Bn*Bs-DARPin9_29. For free doxorubicin IC50 = 441 ± 61 nM, for doxorubicin in the nanoparticles IC50 = 42.7 ± 2.7 nM. Consequently, the incorporation of doxorubicin in the composition of targeted nanoparticles decreases its IC50 by 10.3 times. At the same time, cells exposed to non-targeted PLGA nanoparticles were not affected by the cytotoxic properties of PLGA and survived by more than 82 % even at the highest concentrations of PLGA, namely 1 g/L (Fig. 5d, violet curve). Hence, including a chemotherapeutic drug in the composition of polymer PLGA nanoparticles, assembled on the surface of the cancer cells *via* Barnase*Barstar interface, significantly decreases the concentration of chemotherapeutic drug doxorubicin, needed to receive the same cytotoxic effect.

Discussion

Polymer nanoparticles are the most promising vectors for targeted drug delivery due to their high biocompatibility, a wide spectrum of materials available for synthesis, and the ease of modification with molecules of different origins and functionality[30]. Among the wide range of natural and synthetic polymer materials for the design of therapeutic nanoparticles (such as protein-based polymers, polyphosphates, polyamides, polysaccharides, poly-lactic-co-glycolic acid) PLGA is the most popular polymer commonly used for biomedical and fundamental research application[25]. PLGA has been already approved by FDA for the therapeutic purposes and acts as a unique polymer for drug delivery [31, 32]. PLGA is a co-polymer of fully biocompatible and biodegradable lactic and glycolic acids and has already demonstrated remarkable results in clinical trials as an excellent candidate for drug delivery and treatment [33, 34].

To track the nanoparticles inside the organism, monitor their delivery and biodistribution, and use them for diagnostic tasks, we incorporated the fluorescent dye, namely, Nile Blue into the nanoparticle structure. Nile Blue is a fluorescent dye from the benzophenoxazine family with high fluorescence, high quantum yield, and excellent photostability [35]. The maximum excitation of the dye in dimethyl sulfoxide is 636 nm, and the maximum emission is 669 nm, thus entering the transparency window of biological tissues and making this dye promising for imaging applications *in vivo* [35]. Due to its lipophilic structure, Nile Blue was already used for several biological applications, e.g. for histology *in vitro*. Moreover, several *in*

vivo studies have demonstrated the ability of this dye to accumulate in tumor cells after *i.v.* administration [27, 36]. Despite the above-mentioned advantages and low cost, Nile Blue was unjustly underestimated in biology with a limited number of studies related to its usage.

Here we describe the development of a two-step drug delivery system, based on polymer PLGA nanoparticles possessing both diagnostic and therapeutic properties. The delivery of these nanoparticles to HER2-overexpressing cancer cells is realized *via* proteinaceous Barnase*Barstar interface and HER2-recognizing scaffold protein DARPin9_29. The concept of targeted drug delivery suggests several advantages over standard chemotherapy, such as the decrease of the required dose of a drug, the improved drug penetration into the tumor, and the reduction of side effects [4]. However, the use of traditional targeting molecules for the therapeutics delivery, namely the use of monoclonal antibodies, often leads to a wide spectrum of side effects: i) considerable size of antibodies (150 kDa, 7-14 nm) often does not allow to modify the nanoparticle surface with the required number of IgG molecules for the efficient delivery to cells, ii) post-translational modifications of IgGs require biotechnological production in mammals which is time-consuming and expensive, iii) constant domains of the heavy chains have effector functions that may lead to phagocytosis without participating in the selective target recognizing, or can cause unwanted immunomodulation *in vivo*; iv) the presence of cysteines in the antibody molecule and glycosylation, which play an important structural role [14, 37, 38].

The artificial scaffold polypeptides were used in this study to target the nanoparticles toward cancer cells instead of the traditionally used monoclonal antibodies. In the last two decades, targeted polypeptide scaffold molecules of non-immunoglobulin nature obtained by phage, cellular or ribosomal display technologies, seem to be more effective tools for the delivery of nanoparticles and other substances to the target cells in the tumor site. The most promising synthetic scaffold proteins for the targeted delivery are DARPins (synthetic derivatives of cytoskeleton protein of drosophila – ankyrin) [16, 39–42], monobodies (derivatives of human fibronectin FN3 domain) [43], anticalins (derivatives of lipocalins) [44], avimers (derivatives of extracellular receptor A-domain) [38], affibodies (derivatives of highly stable domain B of staphylococcal protein A) [45] and others. Designed ankyrin repeat protein, or DARPin, was used in this study for the following reasons: it has a small size (14 kDa), high affinity to the molecular target, here receptor HER2 (K_D = 3.8 nM), low immunogenicity, exceptional thermodynamic stability, and absence of cysteines in its structure [16, 46, 47]. Equally important is the ease of large-scale biotechnological production, in contrast to full-size antibodies [16, 48]. All these properties simplify genetic engineering and the creation of multispecific fusion proteins, which allow not only targeting different structures to the cells with certain molecular profiles but also realizing their own diagnostic and therapeutic functions [22, 25, 39, 42, 49]. Here we used DARPin9_29 genetically fused with Barstar which showed highly specific binding to receptor HER2 and allowed us to realize a two-stage delivery system based on Barnase*Barstar interface.

Table 1
The interfaces used for the drug delivery systems with pre-targeting step.

Delivery system	Immunogenicity	Sterical hindrance	Ka	Representation in mammals
Barnase* **Barstar**	✓Both proteins are not immunogenic (unpublished data).	✓Proteins are comparable in size (12 and 10 kDa), and therefore steric hindrances should not arise[23].	10^{14} M^{-1} [50]	✓Both proteins were isolated from bacteria and are not represented in mammals [50].
Streptavidin*biotin	Streptavidin is highly immunogenic [51].	The significant difference in the size (56 kDa and 244 Da) of the molecules can cause steric hindrance: if biotin is bound to a non-smooth surface, then streptavidin will not be able to recognize it. This imposes restrictions on the use of this system in nanomedicine [52–54].	10^{15} M^{-1} [55]	Biotin, or vitamin H, is presented in the blood of mammals which may cause obstacles for appropriate interaction of streptavidin*biotin [56, 57].
Hapten* **antibody**	Antibodies are immunogenic and may have effector functions which make them not the best candidate for long-term treatment [58].	IgG is 150 kDa protein while hapten is a low-molecular compound, so that steric difficulties may arise when the components interact [58, 59].	10^{5}-10^{10} M^{-1} [60]	Antibodies are presented in blood and have effector functions as critical participants in the immune defense [14].

Delivery system	Immunogenicity	Sterical hindrance	Ka	Representation in mammals
Nucleic acids: **i) DNA*DNA** **ii) RNA*RNA** **iii) mirror-imaged oligonucleotides** **iv) phosphorodiamidate morpholino oligomers** **v) peptide nucleic acids** **vi) locked nucleic acid**	✓It was proposed that nucleotides as natural, presented in all organisms molecules with a high charge will be not immunogenic [61]. ✓It was shown that some mirror-imaged oligonucleotides, as well as phosphorodiamidate morpholino oligomers and peptide nucleic acids are not immunogenic [62–65].	Nucleotides are small molecules (less than 500 Da). Since the entire sequence of nucleotides is vital in recognition, it can cause interaction problems if a non-smooth surface is used.	Depends on the base pair number	The presence of nucleases in the serum is an obstacle in the development of the system based on oligonucleotides due to the fast degradation [61]. ✓Due to their artificial origin mirror-imaged oligonucleotides, phosphorodiamidate morpholino oligomers and peptide nucleic acids are resistant to the degradation by the nucleases, peptide and locked nucleic acids are also resistant to protease digestion [63, 65–68].
Click chemistry	✓Molecules used in bioorthogonal chemistry are supposed to be not highly immunogenic [69].	Molecules used in bioorthogonal chemistry are small which can cause interaction problems if a non-smooth surface is used. Also, this approach requires preliminary chemical modification of the delivered molecules, which proceed not completely steric and not with 100% yield.	✓Covalent bonding is stronger than affinity interaction but is not reversible.	✓Molecules used in bioorthogonal chemistry are not represented in mammals [66].

Delivery system	Immunogenicity	Sterical hindrance	Ka	Representation in mammals
SpyTag/ SpyCatcher	N/A	✓Proteins are comparable in size (15 and 13 kDa), and therefore steric hindrances should not arise[70].	✓ Covalent bonding is stronger than affinity interaction but is not reversible.	✓Both proteins were isolated from bacteria and modified by bioengineering and are not represented in mammals [71].

Several two-stage DDSs are currently in use and under development (see Table 1). As shown in Table 1, Barnase*Barstar protein pair outperforms other two-stage systems which makes it a unique tool for the design of multifunctional biomedical products. Barstar (10 kDa) is a natural inhibitor of bacterial ribonuclease Barnase (12 kDa) [23]. These proteins have an extremely high binding affinity (association constant $K_{aff} \sim 10^{14}$ M^{-1}) and fast interaction kinetics (rate constant of complex formation $k_{on} \sim 10^{8}$ $M^{-1}s^{-1}$), at the same time these proteins are not presented in mammals, which allows them to be used in blood flow without any interaction with endogenic components of blood [50, 72]. In the present study, Barstar-DARPin9_29 was used as the first component of the two-stage DDS and nanoparticles modified with Barnase served as the second component. It is also important to note, the lack of immunogenicity of all compounds used here – Barnase, Barstar, and Barstar-DARPin9_29.

Previously we showed the versatility of the Barnase*Barstar protein system for a wide range of applications including targeted delivery of both protein molecules, nanoparticles, and different supramolecular structures. In particular: i) the stability of the Barnase*Barstar protein complex under severe conditions (low pH, high temperature, and presence of chaotropic agents) was demonstrated that opens up more possibilities for using this system in any conditions both *in vitro* and *in vivo* [73]; ii) the successful labeling of HER2-overexpressing cancer cells *in vitro* with the self-assembled structures consisting of the magnetic particles and quantum dots using Barstar and scFv-Barnase-scFv construct (directed toward HER2 antigen) [21] and *in vivo* with radiolabeled 4D5 scFv–Barnase and 4D5 scFv–diBarnase [23] were shown; iii) a universal delivery system based on Barnase-Barstar and SiO_2-binding peptide was developed [25]; iv) bispecific antibodies against HER1 and HER2 antigens using 425scFv-Barstar and 4D5scFv-Barnase [74] were obtained and utilized for imaging of cancer cells with overexpression of these receptors [75]. All the described studies confirm the versatility of the Barnase*Barstar interface for the wide range of biological applications that require the self-assembly of different structures in different conditions. In this work, using Barstar-DARPin9_29 and Barnase-conjugated polymer PLGA nanoparticles loaded with fluorescent dye Nile Blue and chemotherapeutic drug doxorubicin, we showed successful labeling and killing of HER2-overexpressing cells. The use of such two-step DDS allows decreasing the necessary dose of the doxorubicin needed to cause cancer cell death by one level of magnitude.

Conclusions

Here we report the versatile method of the two-stage drug delivery system (DDS) for theranostic applications based on Barnase*Barstar proteinaceous interface. The small size and high affinity constant of these proteins make them an excellent “molecular glue” for the design of different self-assembling structures based on various modules, where one component of this DDS is in the structure of one module (e.g., Barnase in the therapeutic module), and another system component in the structure of another module (e.g., Barstar in targeted DARPin module). This “lego” approach allows escaping such chemical conjugation issues, as non-oriented molecules modification of nanoparticle surface, denaturation of proteins on the nanoparticle surface, conjugation through several functional groups on the same molecule, impossibility of simple replacement of nanoparticle composition. On the contrary, using the proposed platform for nanoparticle biomodification allows obtaining biologically active structures by either mixing components, such as nanoparticle-Barnase + Barstar-DARPin or two-step targeted delivery *in vitro* and *in vivo*. Such a pre-targeting concept allows to significantly reduce the doses of drugs (incorporated into the second toxic component of DDS) to get the same therapeutic effect thus reducing side effects and systemic toxicity. We believe that the proposed system outperforming the existing technologies will promote the development of new-generation drug delivery systems for cancer diagnostics and treatment.

Declarations

Funding

The work was supported in part by the Russian Science Foundation grant № 19-14-00112 (barnase purification) and Russian Foundation for Basic Research № 20-34-70136 (cell culture study), № 19-29-04012 (toxicity study). This study was made possible through the support of the Applied Genetics Resource Facility of MIPT (Support Grant 075-15-2021-684).

Acknowledgments

Not applicable.

Author Information

Victoria Shipunova and Elena Komedchikova contributed equally to this study.

Author Contributions

Conceptualization: V.O.S., M.P.N., S.M.D.; data curation: V.O.S. E.N.K.; formal analysis: V.O.S.; funding acquisition: S.M.D.; investigation: V.O.S.; methodology: V.O.S., M.P.N.; project administration: V.O.S.; resources: V.O.S., M.P.N., S.M.D.; software: A.S.S.; supervision: V.O.S.; validation: V.O.S. E.N.K. P.A.K.; visualization: A.S.S.; writing – original draft: V.O.S., E.N.K., M.P.N. S.M.D.

Ethics declarations

Ethics approval and consent to participate

Not applicable.

Consent for publication

All authors read and approve the final manuscript.

Availability of data and materials

The datasets used and analysed during the current study are available from the corresponding author on reasonable request.

Competing interests

The authors declare that they have no competing interests.

References

1. Sung H, Ferlay J, Siegel RL, Laversanne M, Soerjomataram I, Jemal A, Bray F. Global cancer statistics 2020: GLOBOCAN estimates of incidence and mortality worldwide for 36 cancers in 185 countries. CA Cancer J Clin 2021. doi:10.3322/caac.21660.
2. Carrick S, Parker S, Thornton CE, Ghersi D, Simes J, Wilcken N. Single agent versus combination chemotherapy for metastatic breast cancer. Cochrane Database Syst Rev. 2009:CD003372. doi:10.1002/14651858.CD003372.pub3.
3. Sweeney CJ, Chen Y-H, Carducci M, Liu G, Jarrard DF, Eisenberger M, et al. Chemohormonal Therapy in Metastatic Hormone-Sensitive Prostate Cancer. N Engl J Med. 2015;373:737–46. doi:10.1056/nejmoa1503747.
4. Anselmo AC, Mitragotri S. Nanoparticles in the clinic. Bioeng Transl Med. 2016;1:10–29. doi:10.1002/btm2.10003.
5. Wang AZ, Langer R, Farokhzad OC. Nanoparticle delivery of cancer drugs. Annu Rev Med. 2012;63:185–98. doi:10.1146/annurev-med-040210-162544.
6. Zelepukin IV, Yaremenko AV, Shipunova VO, Babenyshev AV, Balalaeva IV, Nikitin PI, et al. Nanoparticle-based drug delivery via RBC-hitchhiking for the inhibition of lung metastases growth. Nanoscale. 2019;11:1636–46. doi:10.1039/C8NR07730D.
7. Nikitin MP, Zelepukin IV, Shipunova VO, Sokolov IL, Deyev SM, Nikitin PI. Enhancement of the blood-circulation time and performance of nanomedicines via the forced clearance of erythrocytes. Nat Biomed Eng. 2020;4:717–31. doi:10.1038/s41551-020-0581-2.
8. Nikitin MP, Shipunova VO, Deyev SM, Nikitin PI. Biocomputing based on particle disassembly. Nat Nanotechnol. 2014;9:716–22. doi:10.1038/nnano.2014.156.

9. Rivankar S. An overview of doxorubicin formulations in cancer therapy. J Cancer Res Ther. 2014;10:853–8. doi:10.4103/0973-1482.139267.
10. Krauss AC, Gao X, Li L, Manning ML, Patel P, Fu W, et al. FDA Approval Summary: (Daunorubicin and Cytarabine) Liposome for Injection for the Treatment of Adults with High-Risk Acute Myeloid Leukemia. Clin Cancer Res. 2019;25:2685–90. doi:10.1158/1078-0432.CCR-18-2990.
11. Riley RS, June CH, Langer R, Mitchell MJ. Delivery technologies for cancer immunotherapy. Nat Rev Drug Discov. 2019;18:175–96. doi:10.1038/s41573-018-0006-z.
12. Senzer N, Nemunaitis J, Nemunaitis D, Bedell C, Edelman G, Barve M, et al. Phase I study of a systemically delivered p53 nanoparticle in advanced solid tumors. Mol Ther. 2013;21:1096–103. doi:10.1038/mt.2013.32.
13. Hoff DD von, Mita MM, Ramanathan RK, Weiss GJ, Mita AC, LoRusso PM, et al. Phase I Study of PSMA-Targeted Docetaxel-Containing Nanoparticle BIND-014 in Patients with Advanced Solid Tumors. Clin Cancer Res. 2016;22:3157–63. doi:10.1158/1078-0432.CCR-15-2548.
14. Rosenblum D, Joshi N, Tao W, Karp JM, Peer D. Progress and challenges towards targeted delivery of cancer therapeutics. Nat Commun. 2018;9:1410. doi:10.1038/s41467-018-03705-y.
15. Skerra A. Engineered protein scaffolds for molecular recognition. J. Mol. Recognit. 2000;13:167–87. doi:10.1002/1099-1352(200007/08)13:4<167::aid-jmr502>3.0.co;2-9.
16. Binz HK, Amstutz P, Plückthun A. Engineering novel binding proteins from nonimmunoglobulin domains. Nat Biotechnol. 2005;23:1257–68. doi:10.1038/nbt1127.
17. Ståhl S, Gräslund T, Eriksson Karlström A, Frejd FY, Nygren P-Å, Löfblom J. Affibody Molecules in Biotechnological and Medical Applications. Trends in Biotechnology. 2017;35:691–712. doi:10.1016/j.tibtech.2017.04.007.
18. Su X, Yang N, Wittrup KD, Irvine DJ. Synergistic antitumor activity from two-stage delivery of targeted toxins and endosome-disrupting nanoparticles. Biomacromolecules. 2013;14:1093–102. doi:10.1021/bm3019906.
19. Sharkey RM, Karacay H, Cardillo TM, Chang C-H, McBride WJ, Rossi EA, et al. Improving the delivery of radionuclides for imaging and therapy of cancer using pretargeting methods. Clin Cancer Res. 2005;11:7109s-7121s. doi:10.1158/1078-0432.CCR-1004-0009.
20. Marshall D, Pedley RB, Boden JA, Boden R, Melton RG, Begent RH. Polyethylene glycol modification of a galactosylated streptavidin clearing agent: effects on immunogenicity and clearance of a biotinylated anti-tumour antibody. Br J Cancer. 1996;73:565–72. doi:10.1038/bjc.1996.99.
21. Nikitin MP, Zdobnova TA, Lukash SV, Stremovskiy OA, Deyev SM. Protein-assisted self-assembly of multifunctional nanoparticles. Proc Natl Acad Sci U S A. 2010;107:5827–32. doi:10.1073/pnas.1001142107.
22. Shipunova VO, Komedchikova EN, Kotelnikova PA, Zelepukin IV, Schulga AA, Proshkina GM, et al. Dual Regioselective Targeting the Same Receptor in Nanoparticle-Mediated Combination Immuno/Chemotherapy for Enhanced Image-Guided Cancer Treatment. ACS Nano. 2020;14:12781–95. doi:10.1021/acsnano.0c03421.

23. Deyev SM, Waibel R, Lebedenko EN, Schubiger AP, Plückthun A. Design of multivalent complexes using the barnase*barstar module. Nat Biotechnol. 2003;21:1486–92. doi:10.1038/nbt916.
24. Rushizky GW, Greco AE, Hartley RW, Sober HA. STUDIES ON B. SUBTILIS RIBONUCLEASE. I. CHARACTERIZATION OF ENZYMATIC SPECIFICITY. Biochemistry. 1963;2:787–93. doi:10.1021/bi00904a028.
25. Shipunova VO, Zelepukin IV, Stremovskiy OA, Nikitin MP, Care A, Sunna A, et al. Versatile Platform for Nanoparticle Surface Bioengineering Based on SiO2-Binding Peptide and Proteinaceous Barnase*Barstar Interface. ACS Appl Mater Interfaces. 2018;10:17437–47. doi:10.1021/acsami.8b01627.
26. Studier FW. Protein production by auto-induction in high density shaking cultures. Protein Expr Purif. 2005;41:207–34. doi:10.1016/j.pep.2005.01.016.
27. Lin CW, Shulok JR, Kirley SD, Cincotta L, Foley JW. Lysosomal localization and mechanism of uptake of Nile blue photosensitizers in tumor cells. Cancer Res. 1991;51:2710–9.
28. Nitiss JL. Targeting DNA topoisomerase II in cancer chemotherapy. Nat Rev Cancer. 2009;9:338–50. doi:10.1038/nrc2607.
29. Thorn CF, Oshiro C, Marsh S, Hernandez-Boussard T, McLeod H, Klein TE, Altman RB. Doxorubicin pathways: pharmacodynamics and adverse effects. Pharmacogenet Genomics. 2011;21:440–6. doi:10.1097/FPC.0b013e32833ffb56.
30. Masood F. Polymeric nanoparticles for targeted drug delivery system for cancer therapy. Mater Sci Eng C Mater Biol Appl. 2016;60:569–78. doi:10.1016/j.msec.2015.11.067.
31. Pillai O, Panchagnula R. Polymers in drug delivery. Curr Opin Chem Biol. 2001;5:447–51. doi:10.1016/s1367-5931(00)00227-1.
32. Danhier F, Ansorena E, Silva JM, Coco R, Le Breton A, Préat V. PLGA-based nanoparticles: an overview of biomedical applications. J Control Release. 2012;161:505–22. doi:10.1016/j.jconrel.2012.01.043.
33. El-Maghawry E, Tadros MI, Elkheshen SA, Abd-Elbary A. Eudragit®-S100 Coated PLGA Nanoparticles for Colon Targeting of Etoricoxib: Optimization and Pharmacokinetic Assessments in Healthy Human Volunteers. Int J Nanomedicine. 2020;15:3965–80. doi:10.2147/IJN.S244124.
34. Lecio G, Ribeiro FV, Pimentel SP, Reis AA, Da Silva RVC, Nociti-Jr F, et al. Novel 20% doxycycline-loaded PLGA nanospheres as adjunctive therapy in chronic periodontitis in type-2 diabetics: randomized clinical, immune and microbiological trial. Clin Oral Investig. 2020;24:1269–79. doi:10.1007/s00784-019-03005-9.
35. Martinez V, Henary M. Nile Red and Nile Blue: Applications and Syntheses of Structural Analogues. Chemistry. 2016;22:13764–82. doi:10.1002/chem.201601570.
36. LEWIS MR, GOLAND PP, SLOVITER HA. The action of oxazine dyes on tumors in mice. Cancer Res. 1949;9:736–40.
37. Gebauer M, Skerra A. Engineered protein scaffolds as next-generation antibody therapeutics. Curr Opin Chem Biol. 2009;13:245–55. doi:10.1016/j.cbpa.2009.04.627.

38. Silverman J, Liu Q, Lu Q, Bakker A, To W, Duguay A, et al. Multivalent avimer proteins evolved by exon shuffling of a family of human receptor domains. Nat Biotechnol. 2005;23:1556–61. doi:10.1038/nbt1166.
39. Shipunova VO, Shramova EI, Schulga AA, Shilova MV, Deyev SM, Proshkina GM. Delivery of Barnase to Cells in Liposomes Functionalized by Her2-Specific DARPin Module. Russ J Bioorg Chem. 2020;46:1156–61. doi:10.1134/S1068162020060308.
40. Shipunova VO, Kolesnikova OA, Kotelnikova PA, Soloviev VD, Popov AA, Proshkina GM, et al. Comparative Evaluation of Engineered Polypeptide Scaffolds in HER2-Targeting Magnetic Nanocarrier Delivery. ACS Omega. 2021;6:16000–8. doi:10.1021/acsomega.1c01811.
41. Shipunova VO, Kotelnikova PA, Aghayeva UF, Stremovskiy OA, Novikov IA, Schulga AA, et al. Self-assembling nanoparticles biofunctionalized with magnetite-binding protein for the targeted delivery to HER2/neu overexpressing cancer cells. Journal of Magnetism and Magnetic Materials. 2019;469:450–5. doi:10.1016/j.jmmm.2018.09.015.
42. Shramova E, Proshkina G, Shipunova V, Ryabova A, Kamyshinsky R, Konevega A, et al. Dual Targeting of Cancer Cells with DARPin-Based Toxins for Overcoming Tumor Escape. Cancers (Basel) 2020. doi:10.3390/cancers12103014.
43. Koide A, Wojcik J, Gilbreth RN, Hoey RJ, Koide S. Teaching an old scaffold new tricks: monobodies constructed using alternative surfaces of the FN3 scaffold. J Mol Biol. 2012;415:393–405. doi:10.1016/j.jmb.2011.12.019.
44. Beste G, Schmidt FS, Stibora T, Skerra A. Small antibody-like proteins with prescribed ligand specificities derived from the lipocalin fold. Proc Natl Acad Sci U S A. 1999;96:1898–903. doi:10.1073/pnas.96.5.1898.
45. Shipunova VO, Sogomonyan AS, Zelepukin IV, Nikitin MP, Deyev SM. PLGA Nanoparticles Decorated with Anti-HER2 Affibody for Targeted Delivery and Photoinduced Cell Death. Molecules 2021. doi:10.3390/molecules26133955.
46. Steiner D, Forrer P, Plückthun A. Efficient selection of DARPins with sub-nanomolar affinities using SRP phage display. J Mol Biol. 2008;382:1211–27. doi:10.1016/j.jmb.2008.07.085.
47. Deyev S, Vorobyeva A, Schulga A, Proshkina G, Güler R, Löfblom J, et al. Comparative Evaluation of Two DARPin Variants: Effect of Affinity, Size, and Label on Tumor Targeting Properties. Mol Pharm. 2019;16:995–1008. doi:10.1021/acs.molpharmaceut.8b00922.
48. Frejd FY, Kim K-T. Affibody molecules as engineered protein drugs. Exp Mol Med. 2017;49:e306. doi:10.1038/emm.2017.35.
49. Kotelnikova PA, Shipunova VO, Aghayeva UF, Stremovskiy OA, Nikitin MP, Novikov IA, et al. Synthesis of Magnetic Nanoparticles Stabilized by Magnetite-Binding Protein for Targeted Delivery to Cancer Cells. Dokl Biochem Biophys. 2018;481:198–200. doi:10.1134/S1607672918040051.
50. Schreiber G. Methods for studying the interaction of barnase with its inhibitor barstar. Methods Mol Biol. 2001;160:213–26. doi:10.1385/1-59259-233-3:213.

51. Förster GJ, Santos EB, Smith-Jones PM, Zanzonico P, Larson SM. Pretargeted radioimmunotherapy with a single-chain antibody/streptavidin construct and radiolabeled DOTA-biotin: strategies for reduction of the renal dose. J Nucl Med. 2006;47:140–9.
52. Dundas CM, Demonte D, Park S. Streptavidin-biotin technology: improvements and innovations in chemical and biological applications. Appl Microbiol Biotechnol. 2013;97:9343–53. doi:10.1007/s00253-013-5232-z.
53. Huang SC, Stump MD, Weiss R, Caldwell KD. Binding of biotinylated DNA to streptavidin-coated polystyrene latex: effects of chain length and particle size. Anal Biochem. 1996;237:115–22. doi:10.1006/abio.1996.0208.
54. Neish CS, Martin IL, Henderson RM, Edwardson JM. Direct visualization of ligand-protein interactions using atomic force microscopy. Br J Pharmacol. 2002;135:1943–50. doi:10.1038/sj.bjp.0704660.
55. Wilchek M, Bayer EA. [2] Introduction to avidin-biotin technology. In: Avidin-Biotin Technology: Elsevier; 1990. p. 5–13. doi:10.1016/0076-6879(90)84256-g.
56. Rusckowski M, Fogarasi M, Fritz B, Hnatowich DJ. Effect of endogenous biotin on the applications of streptavidin and biotin in mice. Nuclear Medicine and Biology. 1997;24:263–8. doi:10.1016/s0969-8051(97)00061-9.
57. Luong JHT, Male KB, Glennon JD. Biotin interference in immunoassays based on biotin-strept(avidin) chemistry: An emerging threat. Biotechnol Adv. 2019;37:634–41. doi:10.1016/j.biotechadv.2019.03.007.
58. Goldenberg DM. Targeted therapy of cancer with radiolabeled antibodies. J Nucl Med. 2002;43:693–713.
59. Stickney DR, Anderson LD, Slater JB, Ahlem CN, Kirk GA, Schweighardt SA, Frincke JM. Bifunctional antibody: a binary radiopharmaceutical delivery system for imaging colorectal carcinoma. Cancer Res. 1991;51:6650–5.
60. Stéen EJL, Edem PE, Nørregaard K, Jørgensen JT, Shalgunov V, Kjaer A, Herth MM. Pretargeting in nuclear imaging and radionuclide therapy: Improving efficacy of theranostics and nanomedicines. Biomaterials. 2018;179:209–45. doi:10.1016/j.biomaterials.2018.06.021.
61. Kuijpers WH, Bos ES, Kaspersen FM, Veeneman GH, van Boeckel CA. Specific recognition of antibody-oligonucleotide conjugates by radiolabeled antisense nucleotides: a novel approach for two-step radioimmunotherapy of cancer. Bioconjug Chem. 1993;4:94–102. doi:10.1021/bc00019a013.
62. Wlotzka B, Leva S, Eschgfäller B, Burmeister J, Kleinjung F, Kaduk C, et al. In vivo properties of an anti-GnRH Spiegelmer: an example of an oligonucleotide-based therapeutic substance class. Proc Natl Acad Sci U S A. 2002;99:8898–902. doi:10.1073/pnas.132067399.
63. Young BE, Kundu N, Sczepanski JT. Mirror-Image Oligonucleotides: History and Emerging Applications. Chemistry. 2019;25:7981–90. doi:10.1002/chem.201900149.
64. Liu G. A Revisit to the Pretargeting Concept-A Target Conversion. Front Pharmacol. 2018;9:1476. doi:10.3389/fphar.2018.01476.

65. Altai M, Membreno R, Cook B, Tolmachev V, Zeglis BM. Pretargeted Imaging and Therapy. J Nucl Med. 2017;58:1553–9. doi:10.2967/jnumed.117.189944.
66. Patra M, Zarschler K, Pietzsch H-J, Stephan H, Gasser G. New insights into the pretargeting approach to image and treat tumours. Chem Soc Rev. 2016;45:6415–31. doi:10.1039/c5cs00784d.
67. Karkare S, Bhatnagar D. Promising nucleic acid analogs and mimics: characteristic features and applications of PNA, LNA, and morpholino. Appl Microbiol Biotechnol. 2006;71:575–86. doi:10.1007/s00253-006-0434-2.
68. Mallikaratchy P, Gardner J, Nordstrøm LUR, Veomett NJ, McDevitt MR, Heaney ML, Scheinberg DA. A self-assembling short oligonucleotide duplex suitable for pretargeting. Nucleic Acid Ther. 2013;23:289–99. doi:10.1089/nat.2013.0425.
69. van de Watering FCJ, Rijpkema M, Robillard M, Oyen WJG, Boerman OC. Pretargeted imaging and radioimmunotherapy of cancer using antibodies and bioorthogonal chemistry. Front Med (Lausanne). 2014;1:44. doi:10.3389/fmed.2014.00044.
70. Bae Y, Kim GJ, Kim H, Park SG, Jung HS, Kang S. Engineering Tunable Dual Functional Protein Cage Nanoparticles Using Bacterial Superglue. Biomacromolecules. 2018;19:2896–904. doi:10.1021/acs.biomac.8b00457.
71. Zakeri B, Fierer JO, Celik E, Chittock EC, Schwarz-Linek U, Moy VT, Howarth M. Peptide tag forming a rapid covalent bond to a protein, through engineering a bacterial adhesin. Proc Natl Acad Sci U S A. 2012;109:E690-7. doi:10.1073/pnas.1115485109.
72. Schreiber G, Fersht AR. Energetics of protein-protein interactions: Analysis ofthe Barnase-Barstar interface by single mutations and double mutant cycles. J Mol Biol. 1995;248:478–86. doi:10.1016/s0022-2836(95)80064-6.
73. Aghayeva UF, Nikitin MP, Lukash SV, Deyev SM. Denaturation-resistant bifunctional colloidal superstructures assembled via the proteinaceous barnase-barstar interface. ACS Nano. 2013;7:950–61. doi:10.1021/nn302546v.
74. Semenyuk EG, Stremovskiy OA, Edelweiss EF, Shirshikova OV, Balandin TG, Buryanov YI, Deyev SM. Expression of single-chain antibody-barstar fusion in plants. Biochimie. 2007;89:31–8. doi:10.1016/j.biochi.2006.07.012.
75. Zdobnova TA, Stremovskiy OA, Lebedenko EN, Deyev SM. Self-assembling complexes of quantum dots and scFv antibodies for cancer cell targeting and imaging. PLoS One. 2012;7:e48248. doi:10.1371/journal.pone.0048248.

Figures

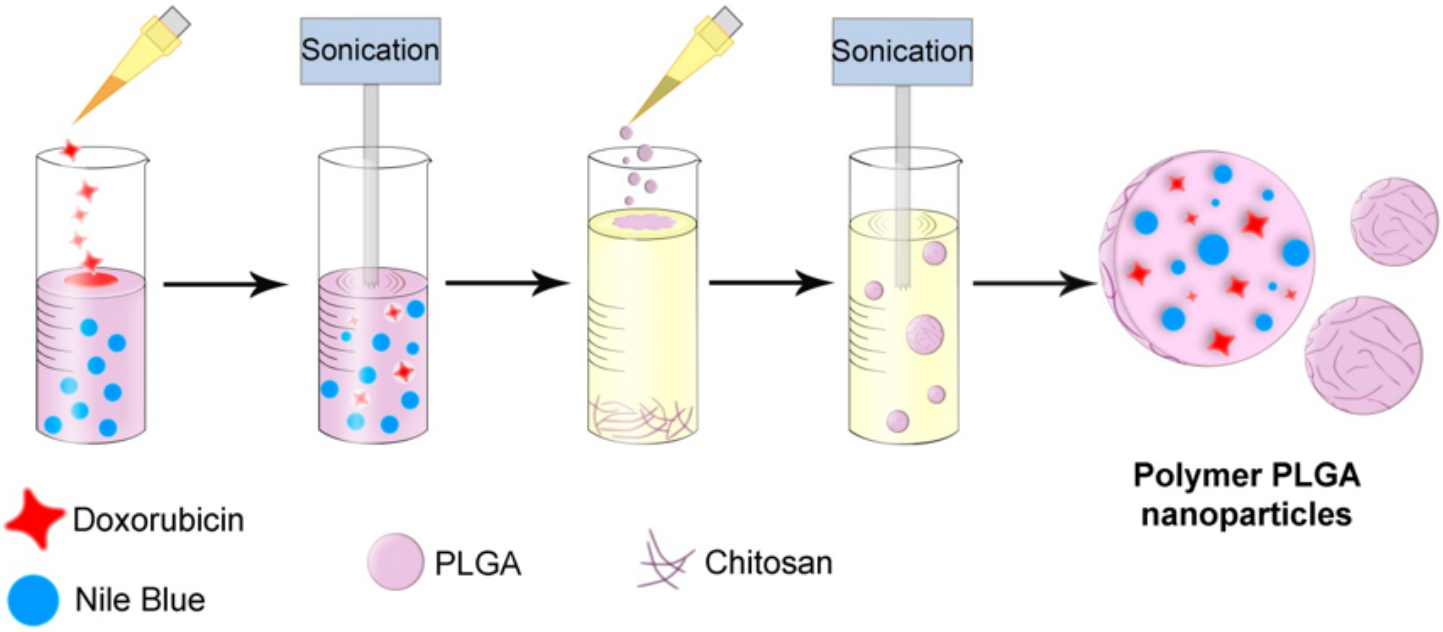

Figure 1

Schematic illustration of polymer nanoparticle synthesis by double emulsion method. The first emulsion was produced by sonication of doxorubicin water solution and solution of PLGA and Nile Blue in chloroform. The second emulsion was created by adding the first emulsion to the polyvinyl alcohol (PVA) and chitosan oligosaccharide lactate water solution. Next, the as-obtained suspension was centrifuged thrice and thus colloidally stable polymer PLGA nanoparticles were obtained.

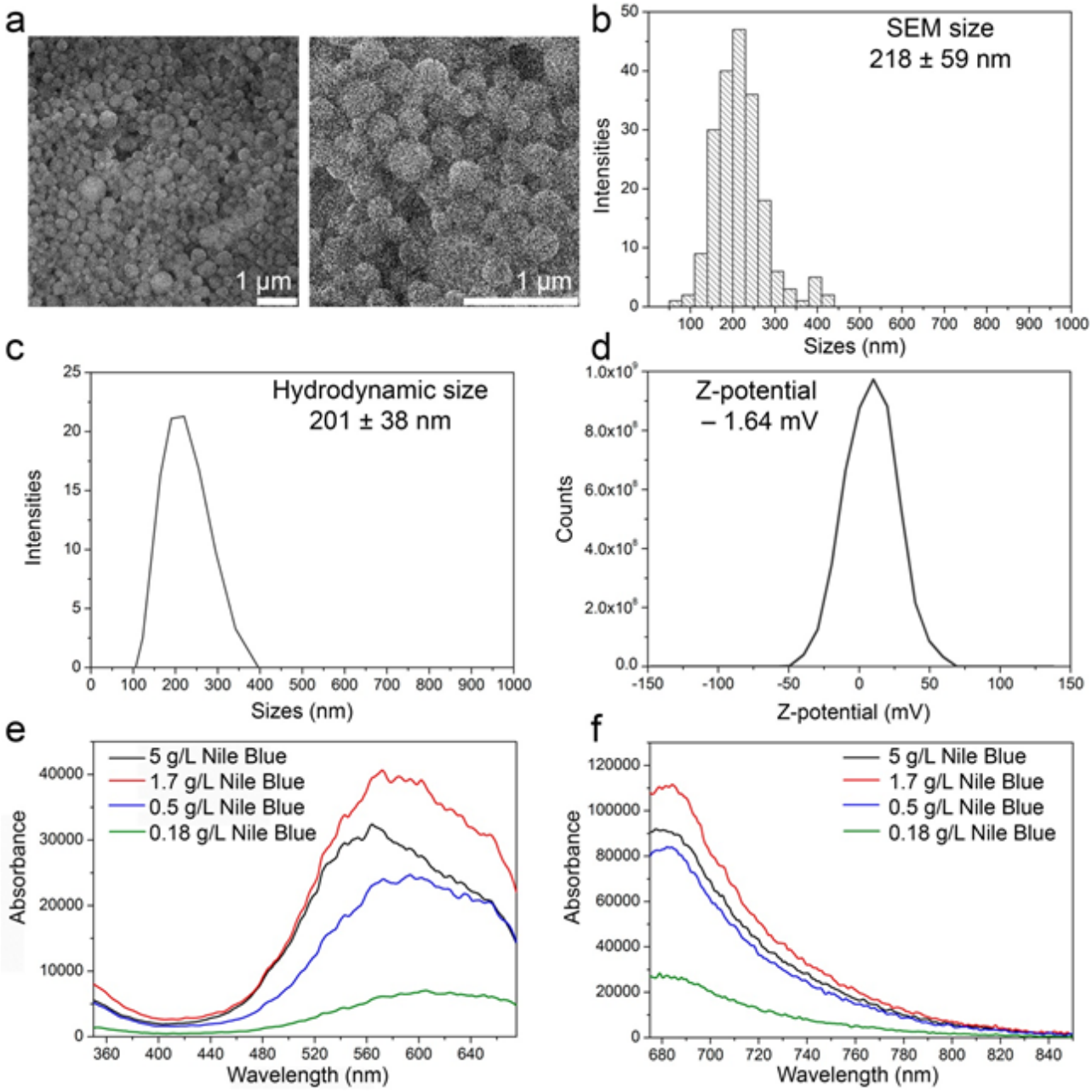

Figure 2

Physico-chemical properties of PLGA nanoparticles. (a) Scanning electron microscopy microphotograph. (b) The physical size distribution of nanoparticles, obtained by image processing. (c) Hydrodynamic size distribution was obtained by the dynamic light scattering method. (d) ζ-potential distribution of nanoparticles obtained by the electrophoretic light scattering method. (e) The excitation spectra (emission wavelength 700 nm) of PLGA nanoparticles according to the fluorescent dye concentration. (f) The emission spectra (excitation wavelength 650 nm) of PLGA nanoparticles according to fluorescent dye concentration.

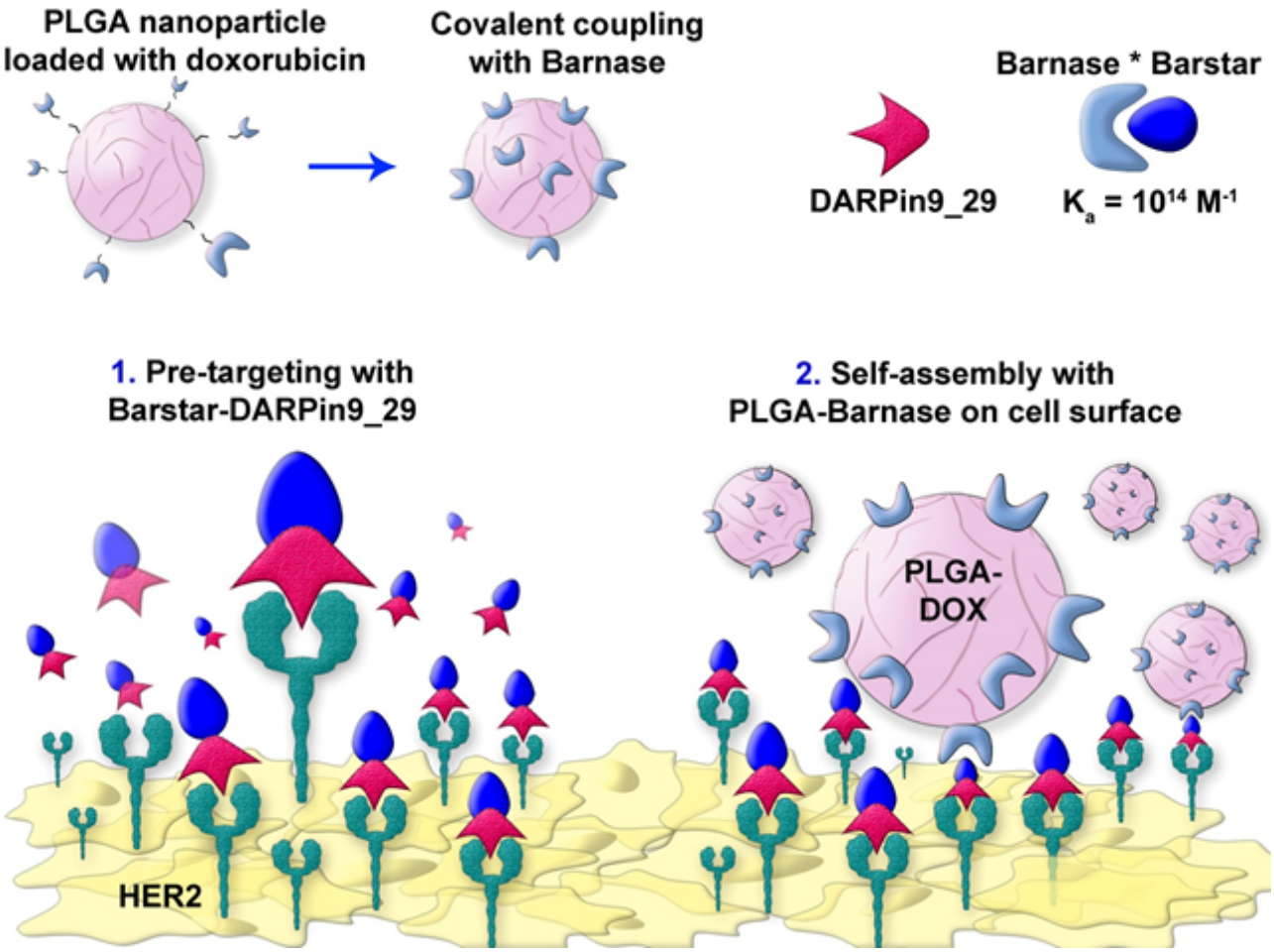

Figure 3

The scheme of the self-assembly of nanoparticles with scaffold polypeptides using protein interface Barnase*Barstar for the delivery to HER2-overexpressing cancer cells. The surface of nanoparticles is covalently modified with one of the adapters, Barnase, then the structure is assembled with Barstar, the second component of the pair, which is fused with targeting scaffold protein DARPin9_29. DARPin9_29 selectively recognizes receptor HER2 on the surface of cancer cells. This modular approach allows using the system for the assembly of different types of nanoparticles and target molecules.

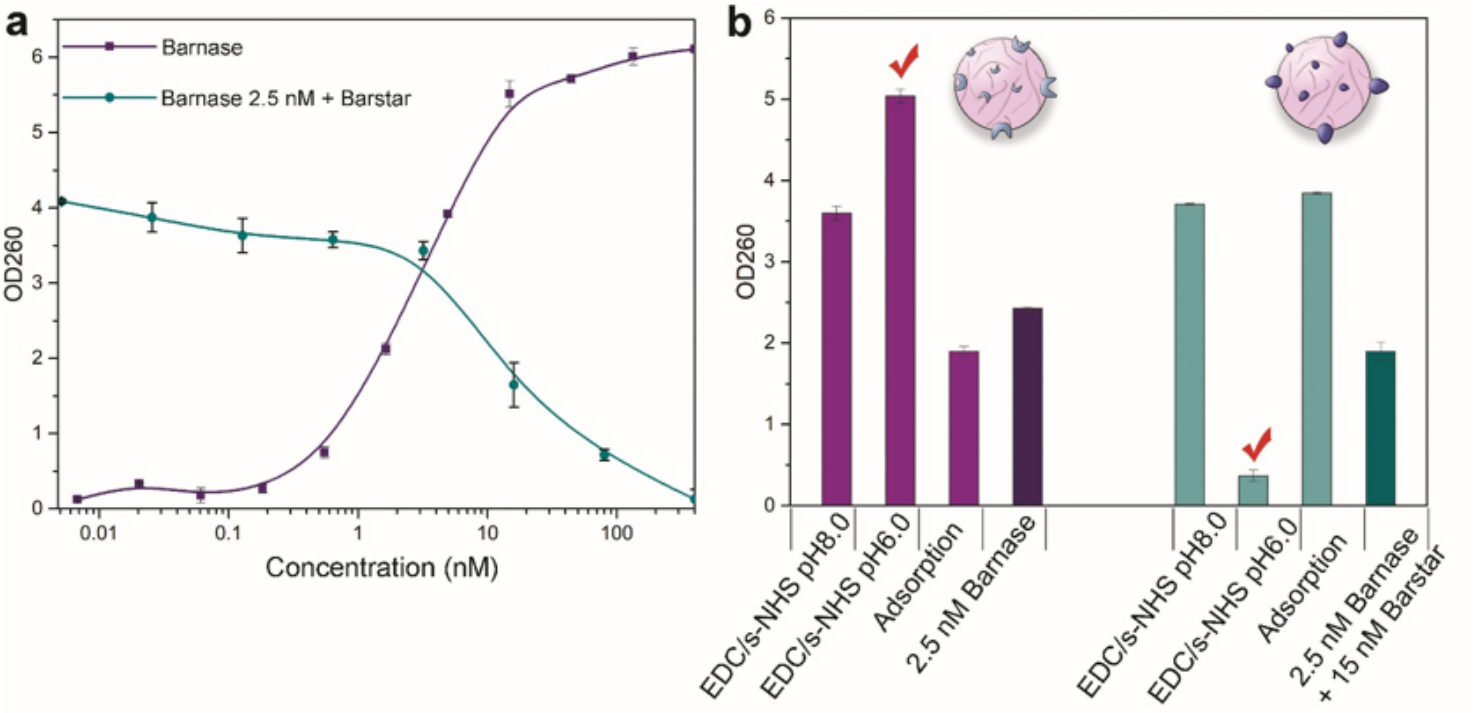

Figure 4

Functional activity of PLGA nanoparticles conjugated with Barnase and Barstar proteins. (a) The enzymatic activity of Barnase (purple curve) and Barstar (green curve) versus protein concentration. (b) The enzymatic activity of PLGA conjugates with Barnase (purple bars) and Barstar (green bars). Data is presented for conjugates obtained at pH 8.0, pH 6.0, and by protein absorption on the particle surface. Optical density (OD260) corresponded to the concentration of free mononucleotides was measured at a wavelength of 260 nm.

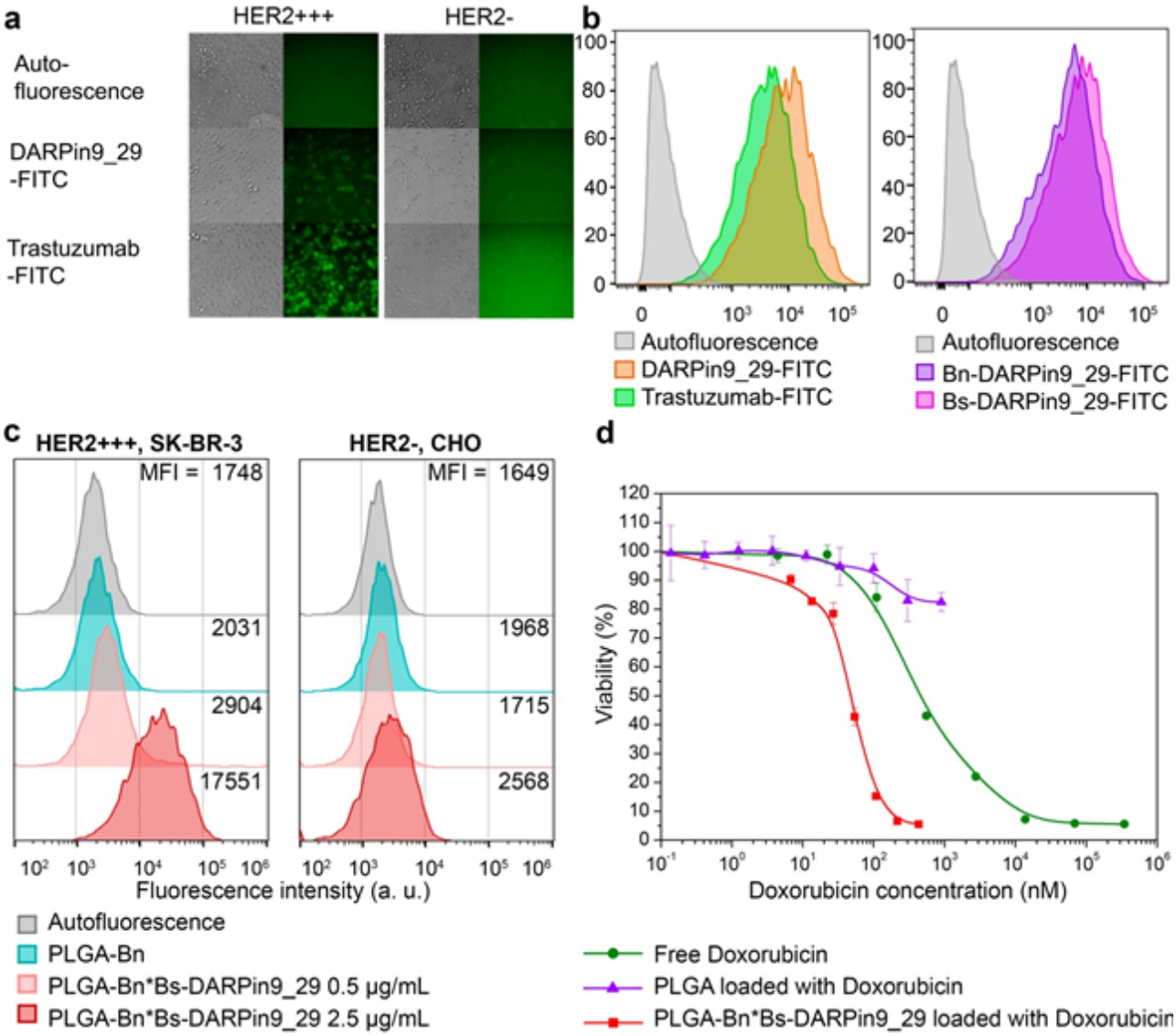

Figure 5

Targeted delivery and cytotoxicity of PLGA-Bn*Bs-DARPin9_29 nanostructures. (a) Fluorescent microscopy of SK-BR-3 and CHO cells, labelled with Trastuzumab-FITC and DARPin9_29-FITC. Left panels – bright-field images, right panels – fluorescent images of the cells. (b) Flow cytometry of SK-BR-3 cells, labelled with DARPin9_29-FITC, Trastuzumab-FITC, Bn-DARPin9_29-FITC, and Bs-DARPin9_29-FITC in the fluorescence channel FL1 corresponding to FITC fluorescence. (c) Flow cytometry of SK-BR-3 and CHO cells, labelled with PLGA-Bn*Bs-DARPin9_29 nanostructures in the fluorescence channel FL4 corresponding to Nile Blue fluorescence. (d) Cytotoxicity of free doxorubicin and doxorubicin in the composition of PLGA and PLGA-Bn*Bs-DARPin9_29 obtained with MTT assay.

Supplementary Files

This is a list of supplementary files associated with this preprint. Click to download.

- GraphicalAbstract.png